AD-A065 884 INSTITUTE FOR ACOUSTICAL RESEARCH MIAMI FLA F/G 8/3
BEAR BUOY STUDY. INTERNAL WAVE MODE PERTURBATIONS DUE TO THE PA--ETC(U)
NOV 78 K L ECHTERNACHT N00014-74-C-0229
UNCLASSIFIED IAR-78004 NL

1 OF 1
ADA
065884

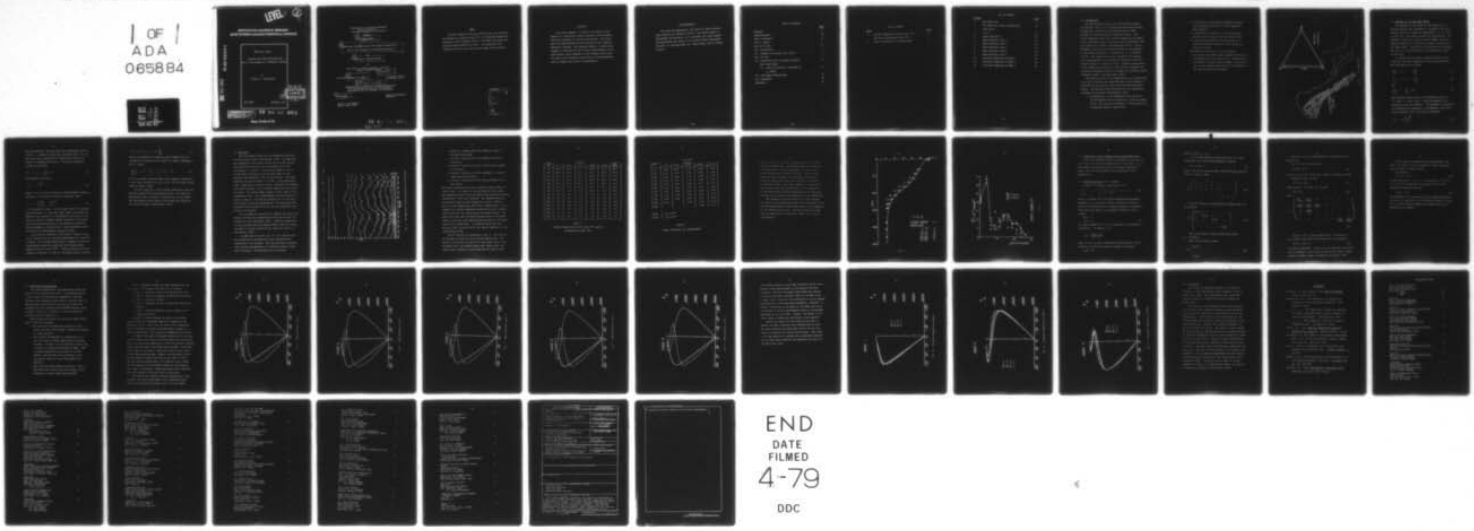

END
DATE
FILMED
4-79
DDC

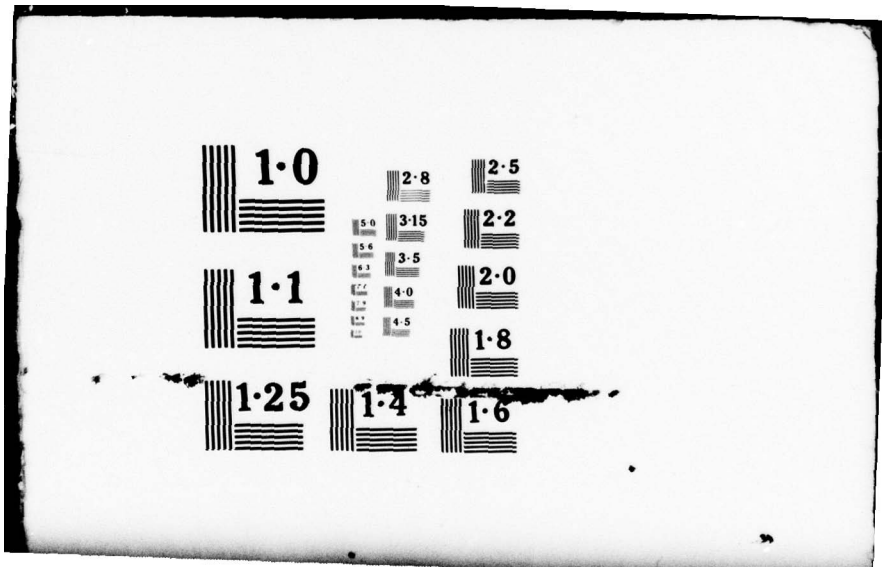
1·0
1·1
1·25
1·4
1·6
1·8
2·0
2·2
2·5
2·8
3·15
3·5
4·0
4·5
5·0
5·6
6·3

INSTITUTE FOR ACOUSTICAL RESEARCH
MIAMI DIVISION PALISADES GEOPHYSICAL INSTITUTE

BEAR Buoy Study:

Internal Wave Mode Perturbations Due to the Passage of a Mesoscale Feature

by

Kenneth L. Echternacht

IAR 78004

November 1978

Miami, Florida 33130

Institute for Acoustical Research
Miami Division of
Palisades Geophysical Institute

(11) Report

November 1978

(6) BEAR Buoy Study: Internal Wave Mode Perturbations Due to the Passage of a Mesoscale Feature

by

(10) Kenneth L. Echternacht

to

The Office of Naval Research, Code 222
Sensor Systems Program

(12) 47 p.

(15) Contract: N00014-74-C-0229

2 October 1978 to
27 October 1978

(9) Final rept.,

(14) IAR-78004

Morton Kronengold,
Director

615 S.W. 2nd Avenue
Miami, Fla. 33130

NOTE

The work reported here was carried out at the Institute for Acoustical Research, Miami Div. of Palisades Geophysical Institute, from 2 October 1978 to 27 October 1978 under ONR Contract Number N00014-74-C-0229. "No inventions were conceived or first put into practice under this contract".

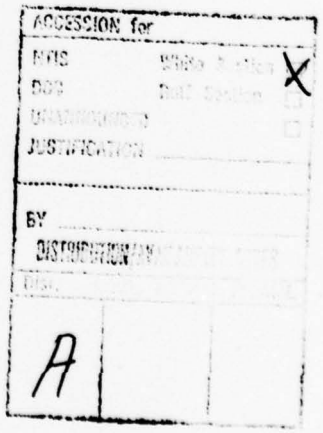

Abstract

This study examines, in detail, the effect of the passage of a meso-scale feature through an area normally under the influence of the Antilles Current. The study area lies approximately 40 km northeast of the island of Eleuthera, Bahamas. The analyses examine, in particular, changes in structure of the vertical displacements of the semi-diurnal tidal component of the internal wave field. The report also includes a description of the methodology used to compute the vertical displacements.

Acknowledgments

This work was supported by the Office of Naval Research under contract No. N00014-74-C-0229. The author wishes to acknowledge the following I.A.R. personnel for their support and help during the course of this study: Morton Kronengold, Director, Dr. William Jobst, Mr. James Doubek, and Ms. Martha Prohias.

Table of Contents

List of Tables

List of Figures

1.0 Introduction

The observations used in this and a previous study (Echternacht, 1978) were acquired over the period February through April 1976 using the BEAR Buoy System (BEAR acronymn for Bermuda Eleuthera Acoustics Range). The system comprised a semi-taut surface buoyed mooring system using a thermistor cable to measure ocean temperatures from near surface to a depth of approximately 1900 m. The experimental site was located approximately 40 Km northeast of the island of Eleuthera, Bahamas (Fig. 1) at $25^{o}45'N$, $76^{o}17'W$. The anchor position was located on the abyssal plain approximately 20 Km seaward of the base of the continental slope at a depth of 4797 m. Detailed descriptions of the system and components as well as data reduction and correction techniques used can be found in Echternacht (1976), Kronengold (1976), and Echternacht (1977).

The primary intent of the experiment was to provide data to be used to examine the amplitude and relative changes in amplitude of the internal tides along the Eleuthera shelf region. The previous report dealing with the observations presented the following (Echternacht, 1978).

1. An examination of the temperature time series at various depths from near surface to below the thermocline. The time series covered a 51 day period from 16 February through 6 April 1976.

2. A discussion of the depth and temporal changes of the observed profiles of static stability - Brunt-Väisälä.
3. A discussion of changes in the internal semi-diurnal tidal field over the period of record.
4. A qualitative discussion of the passage of a meso-scale feature through the area during the period of record.

The intent of this study is the following.

1. To present the method used to compute the vertical displacements for the (baroclinic) internal modes.
2. To examine in greater detail changes in the structure of the internal modes due to the influence of the observed meso-scale feature.

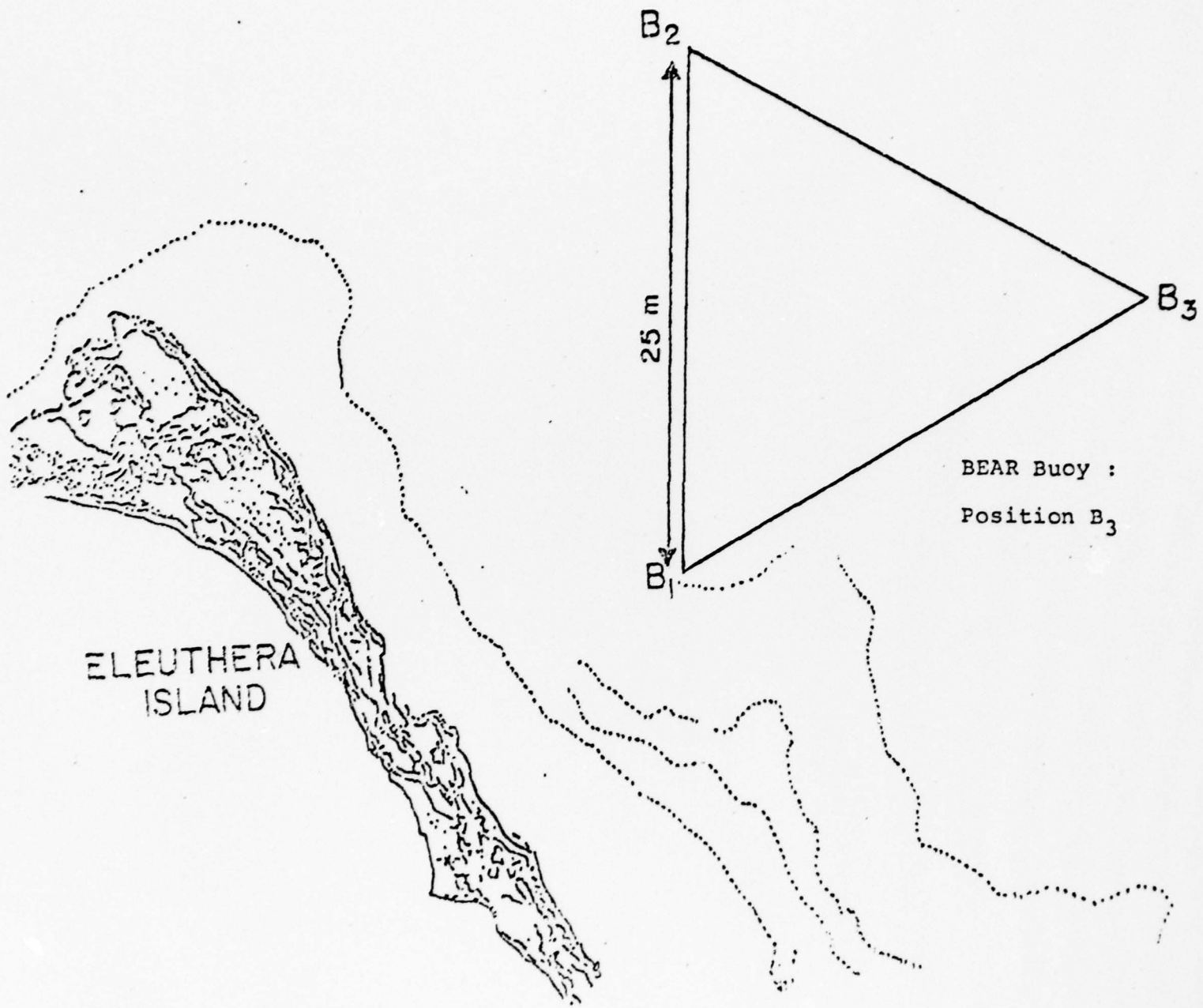

Fig. 1 The Study Area

2.0 Synopsis of Internal Wave Theory

The emphasis of this study is the examination of internal motions with frequency, σ, bounded by the local inertial and static stability frequencies; i.e., $f < \sigma < N$. In particular, this study examines the semi-diurnal tidal frequency, primarily, because internal tidal waves are commonly observed to be the most energetic, especially in the study region. The theory to be presented is intended, strictly, as a recapitulation of the established theory in this area.

In considering the above internal motions for the study area the basic equations of motion representative mid-latitudes are as follows.

$$\frac{\partial u}{\partial t} - fv = -\frac{\partial P}{\partial x} \tag{1}$$

$$\frac{\partial v}{\partial t} + fu = -\frac{\partial P}{\partial y} \tag{2}$$

and

$$\frac{\partial w}{\partial t} = -\frac{\partial P}{\partial z} + b \tag{3}$$

The coordinate system used is of standard notation; ie (x - east, v - north, and z - vertical downward with reference to the sea surface). The parameter b represents the fluctuation in buoyancy, p the departure from hydrostatic pressure, and f the Coriolis parameter

$$b = -g\frac{\rho - \bar{\rho}}{\bar{\rho}} \tag{4}$$

The bar represents the mean and g the acceleration due to gravity. It should be noted that the above (Eqs. 1-3) are the linearized, nondissipative equations of motion and assume an incompressible ocean. The latter assumption yields the following.

$$\frac{\partial u}{\partial x} + \frac{\partial v}{\partial y} + \frac{\partial w}{\partial z} = 0 \tag{5}$$

The buoyancy equation is

$$\frac{\partial b}{\partial t} + w N^2 = 0 \tag{6}$$

where, N is the static stability or Brunt-Väisälä frequency. Typically, N is defined as follows (Phillips, 1966).

$$N^2 = -\frac{g}{\bar{\rho}} \frac{d\bar{\rho}}{dz} - \left(\frac{g}{c}\right)^2 \tag{7}$$

c is the speed of sound. For the study area N^2 is strongly depth dependent. In the water layer above the thermocline ($<$1000 m) the stability is influenced by variations in the Antilles Current, seasonal changes occurring in the mixed layer and perturbations due to the passage of mesoscale eddies embedded in the mean flow. Below thermocline depth the waters are approximately neutrally stable.

Of particular interest in the study of internal waves is the structure of the vertical displacement as a function of depth. The standard method used to compute the vertical displacements seeks wave solutions which assume simple harmonic motion in time ($e^{i\sigma t}$). After differentiation with respect to time Eqs. (3) and (6) are added together forming:

$$(N^2 - \sigma^2) w = -i\sigma \frac{\partial P}{\partial z} \tag{7}$$

Using an eigenfunction expansion which assumes that the variables are separable with respect to spatial dependency Eq (7) yields:

$$\frac{d^2 W}{dz^2} + k^2 \left(\frac{N^2 - \sigma^2}{\sigma^2 - f^2} \right) w = 0 \tag{8}$$

k^2 is an unknown eigenvalue, For a more complete discussion of the steps involved to arrive at Eq. (8) the reader should refer to Mooers (1975).

For this study Eq. (8) was solved numerically using N^2 profiles computed from environmental data. The numerical methodology used is treated in Section 4.0 of this report. The environmental data used for this study were presented in an earlier report (Echternacht, 1978).

3.0 The Data

The environmental data were presented and discussed in the previous report (Echternacht, 1978). To summarize, the temperature time series covered the 51.5 day period from 1200 LST Julian Day (JD) 46 through JD 97, 1976 (15 February - 6 April). The data are shown in Fig. 2. In the figure the axes are Julian Days (time) on the abscissa and temperature (^{o}c) on the ordinate. The same ordinate scaling was used for all data. Each temperature trace, comprised of 3-hourly values, represents the temperature which occurred at the corrected depth over the period of record. The sensor number appears to the right of each temperature trace. The corresponding corrected depths are given in Table 1. The obvious features are (1) the meso-scale feature covering approximately a 24 day period from the start of the record to JD 70, and (2) pronounced semi-diurnal oscillations.

In an attempt to qualitatively classify the meso-scale feature the data were compared with the Ring Criteria defined by Lai and Richardson (1977). From that comparison it was concluded that the observed feature was most likely the edge of an eddy traversing the study area (refer to Echternacht, 1978).

In examining the record (Fig. 2) it is obvious that the occurence of the meso-scale event introduces non-stationarity into the data. Thus the data were segmented into sections representative of different stages of meso-scale influence. The sectioning was as follows.

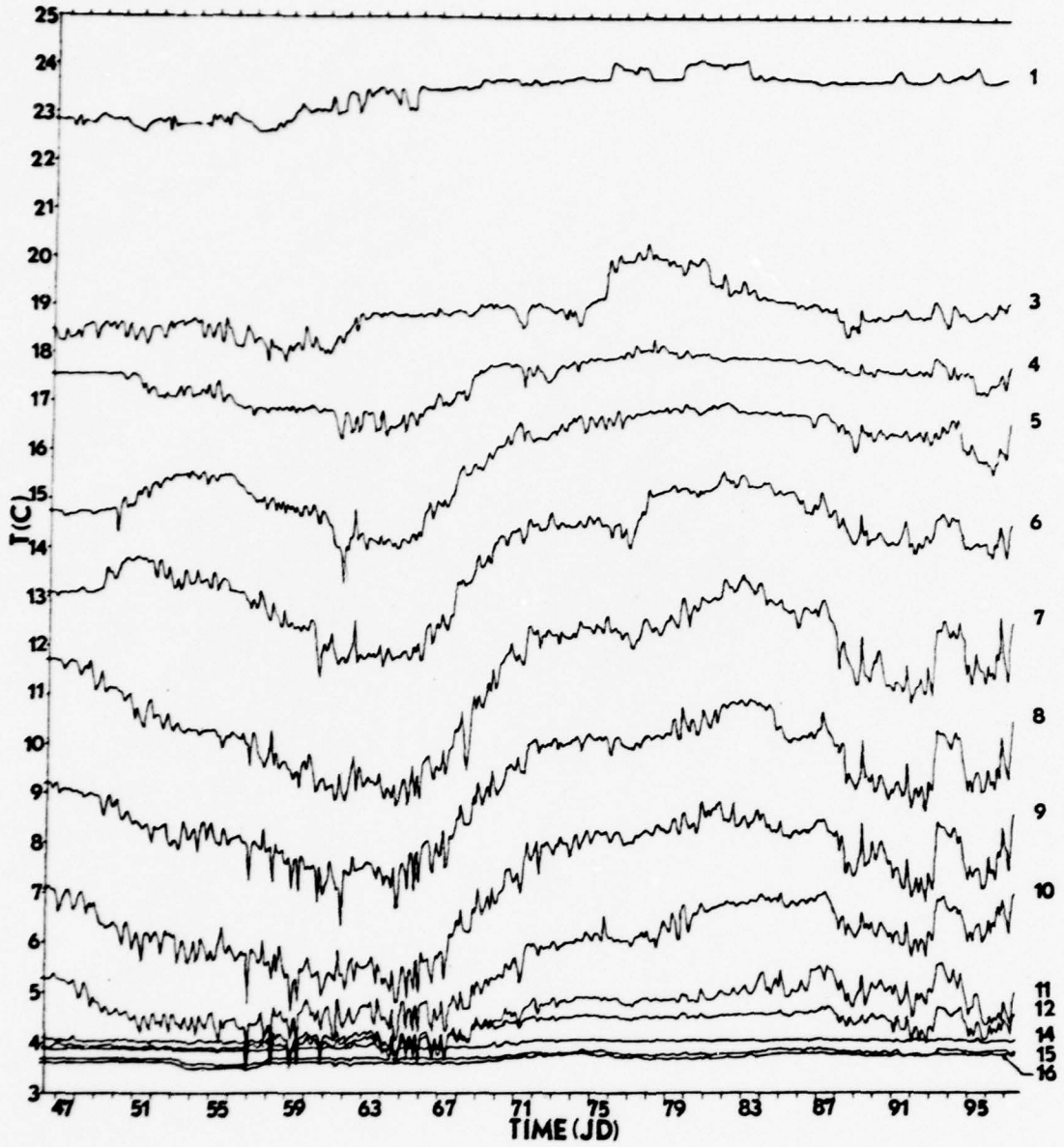

Fig. 2 The BEAR Buoy 3-hourly Temperature Time Series

1. Section 1 covering JD 47-57: period of onset of the meso-scale event.
2. Section 2 covering JD 57-69: period of greatest perturbing.
3. Section 3 covering JD 69-76: period of the passage of the event.
4. Section 4 covering JD 76-88: quiescent - no observable meso-scale feature.
5. Section 5 covering JD 88-97: minor perturbation in the record.

The above sectioning was used to study the above listed as static cases. To arrive at the data base for this study the temperature and N^2 profiles used in the previous analyses (Echternacht, 1978) were averaged. The averaged data and the profiles used for each average are given in Tables 1 and 2 for the temperature and N^2 data, respectively. Fig. 3 compares the average temperature profiles with the climatological mean for the region during the winter season. The meso-scale event had a decided cooling effect on the water column in the zone from approximately the base of the mixed layer to the thermocline. It should be noted that the Section 4 data (profiles 16-20) are nearly identical to the climatological mean.

The N^2 sections are presented in Fig. 4. The trace in the diagram is given for the quiescent period only. For period 4 the profile is typical for the winter case in the Eleuthera area: the shallow mixed layer stable zone, the stable layer centered in and around 600-700 m due to the

Depth (m)	Profile 1-5	6-11	12-15	16-20	21-25	Clim. Mean
22	22.8	23.2	23.7	23.8	23.7	22.3
250	18.5	18.6	19.1	19.5	18.8	19.0
350	17.3	16.8	17.8	18.0	17.6	17.8
450	15.1	14.6	16.4	16.8	16.3	16.6
550	13.3	12.3	14.3	15.1	14.3	15.2
650	10.6	9.5	12.0	12.8	11.7	13.0
750	8.4	7.6	9.8	10.4	9.5	10.4
850	6.1	5.6	7.7	8.4	7.7	8.2
950	4.6	4.5	5.8	6.6	6.3	6.7
1050	4.0	4.0	4.7	5.0	5.0	5.6
1150	3.9	4.0	4.5	4.5	4.4	4.9
1480	3.9	3.9	4.0	4.0	4.0	4.2
1650	3.7	3.7	3.8	3.8	3.8	4.1
1830	3.6	3.6	3.7	3.7	3.8	3.9

Table 1

Average Temperature Profile Data (^{o}C) and the

Climatological Mean (^{o}C)

$N^2 \times 10^{-5}$

Depth	Profile 1-5	6-11	12-15	16-20	21-25
22	3.88	4.29	4.31	4.03	4.60
150	6.12	6.62	6.67	6.28	6.99
250	0.93	2.26	1.34	1.90	0.91
350	2.99	2.91	1.32	0.84	1.27
450	1.13	2.16	1.89	1.17	1.72
550	2.63	2.49	1.99	2.31	2.60
650	1.92	1.08	2.24	2.58	2.08
750	1.47	1.10	1.53	1.59	1.07
850	0.89	0.43	1.65	1.57	0.82
950	0.07		0.45	1.03	0.67
1050				0.28	0.33
2000	1.0×10^{-6}				
5000	1.0×10^{-8}				

Table 2

Static Stability: N^2 $(\text{radians/sec})^2$

Antilles Current, and near neutral stability at depths below the thermocline. For periods under the influence of the meso-scale feature (Sections 1-3) there exist noted perturbations in the N^2 profile. The most noteworthy are the formation of a secondary stable layer below the mixed layer zone and a decrease in stability in 600-700 m layer. The latter suggests a weakening of the effect of the Antilles Current by the introduction of the waters with different properties or at least differences in the vertical distribution of those properties.

The analyses to follow (Section 5.0) will present the effect of the meso-scale event on the structure of the vertical displacements of the semi-diurnal tidal component of the internal wave field. The next section will deal with the method used to numerical compute the vertical displacements.

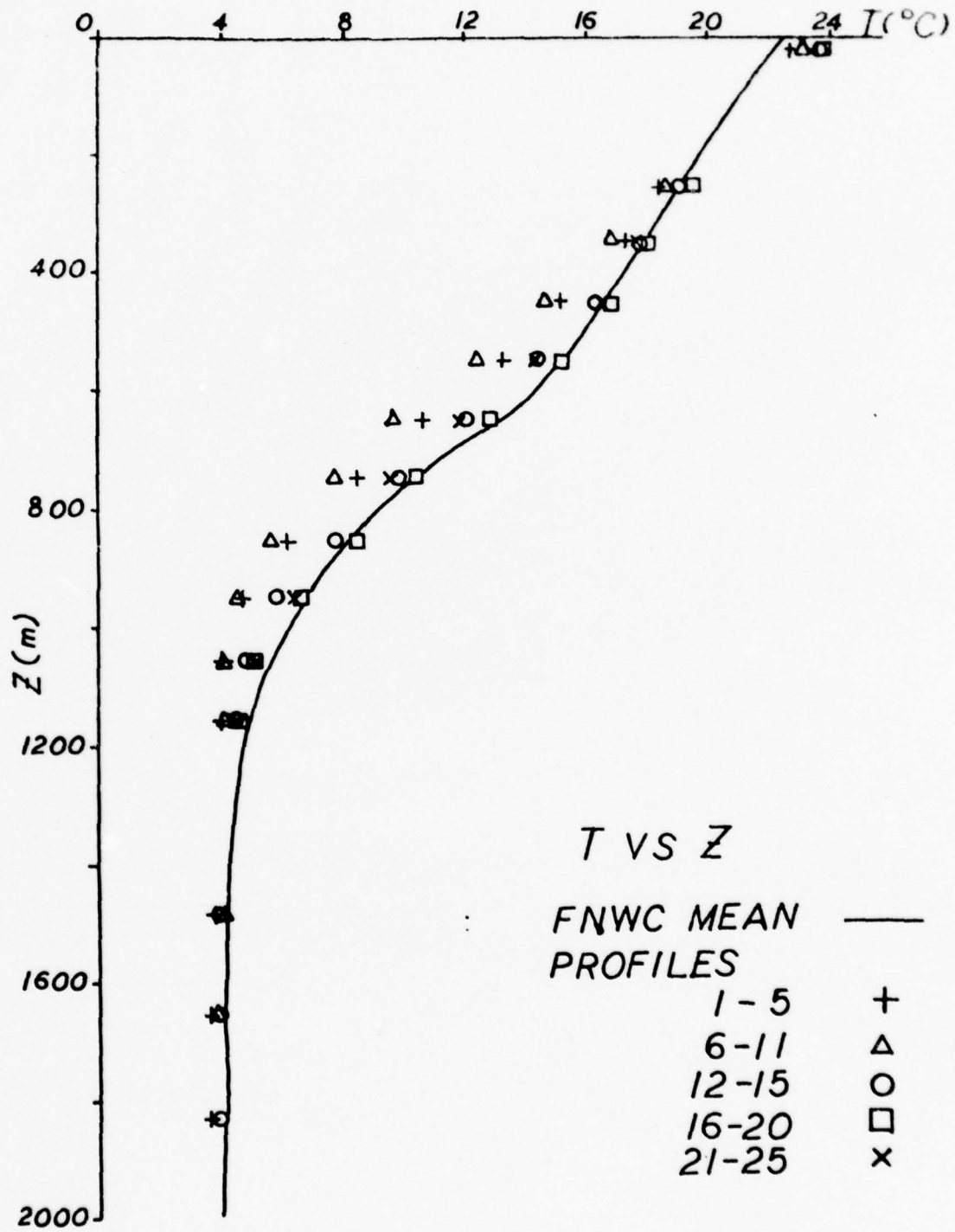
0
4
8
12
16
20
24
T(°C)
400
800
1200
1600
2000
Z(m)
T VS Z
FNWC MEAN PROFILES
1-5 +
6-11 △
12-15 ○
16-20 □
21-25 ×

Fig. 3

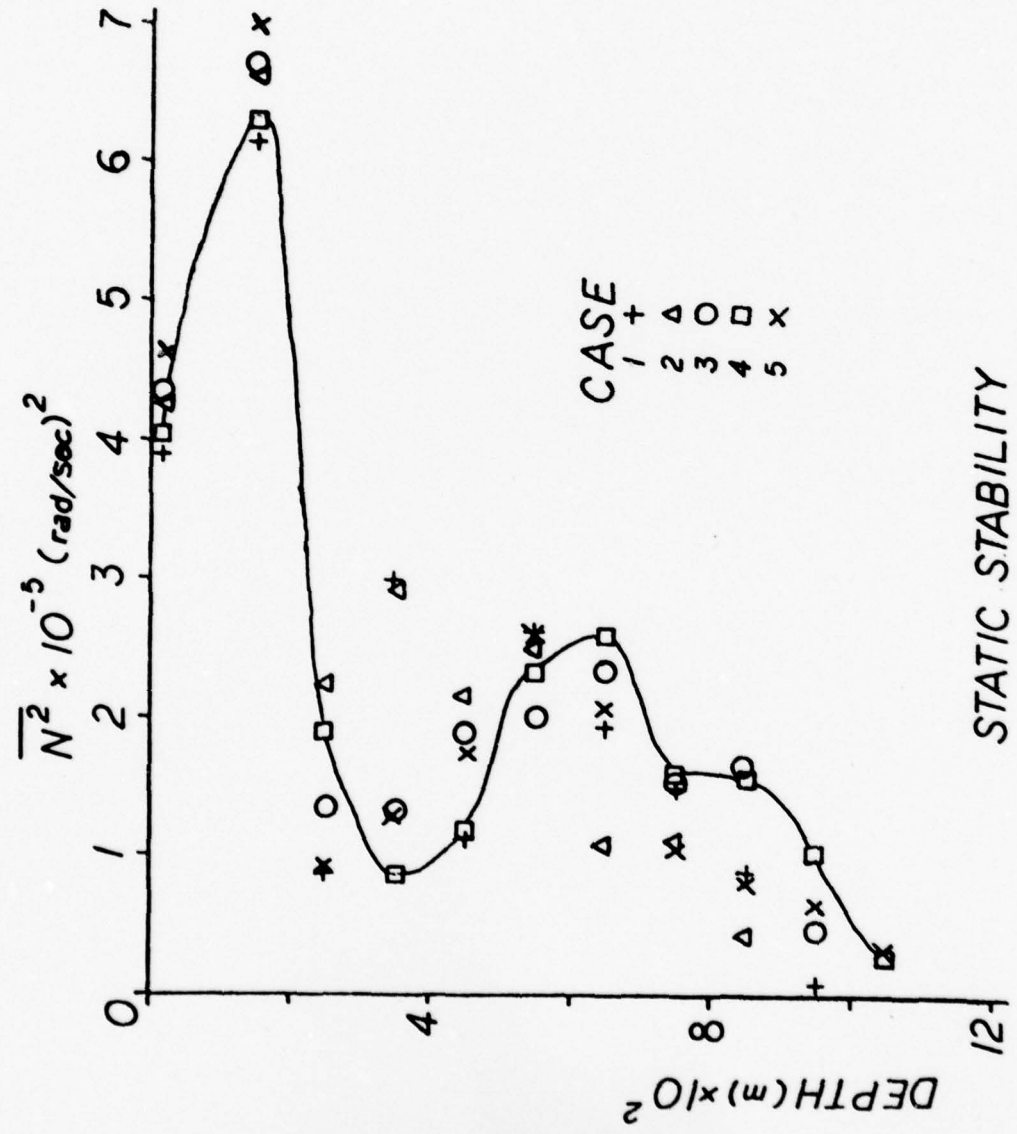
$\overline{N^2} \times 10^{-5}$ (rad/sec)^2
0
1
2
3
4
5
6
7
DEPTH (m) x10^2
0
4
8
12
CASE
1 +
2 Δ
3 O
4 □
5 x
STATIC STABILITY

Fig. 4

4.0 Methodology Used to Compute Internal Wave Mode Shapes

Using the computed N^2 profiles presented in the previous section Eq. (8) was solved numerically to yield the vertical displacement eigenfunctions for the internal (baroclinic) modes. The following presents the description of the methodology.

4.1 Method Description by J. Doubek

We have the equation (from Section 2.0)

$$\frac{d^2 w}{dz^2} + k^2 \left(\frac{N^2(z) - \sigma^2}{\sigma^2 - f^2} \right) w(z) = 0 \qquad (8)$$

where z is depth, $N^2(z)$ the depth dependent Brunt-Väisälä frequency, f is the local inertial frequency, σ the frequency of interest and k^2 an unknown parameter (eigenvalue). Given the water depth D, the boundary conditions are as follows

$$w(0) = 0$$

$$w(D) = 0. \qquad (9)$$

The above assumes $N^2 > \sigma^2 > f^2$; ie applicable to intermediate frequencies. To simplify, let

$$g(z) = \frac{N^2(z) - \sigma^2}{\sigma^2 - f^2} .$$

Then, if g(z) is twice continucusly differentiable, there exists an infinite but countable number of solutions

$$w_n(z), \; k_n^2$$

where $0 < k_1^2 < k_2 \ldots < k_n$.

To solve the boundary value problem Eq. (8) is approximated using the finite difference equation

$$D\bar{u} + \lambda^2 B\bar{u} = 0 \tag{10}$$

where D is the second order NxN finite difference operator (refer to Keller, 1968).

$$D = \begin{pmatrix} -2 & 1 & 0 & 0 & \cdots & & \\ 1 & -2 & 1 & 0 & 0 & \cdots & \\ 0 & 1 & -2 & 1 & 0 & \cdots & \\ & & & \cdot & \cdots & & \\ & & & \cdot & \cdots & 0 & 1 & -2 \end{pmatrix} \tag{11}$$

λ^2 is k^2 scaled by a discretization constant and B is the operator

$$B = \begin{pmatrix} g(z_1) & 0 & 0 & \cdots & & & \\ 0 & g(z_2) & 0 & \cdots & & & \\ 0 & 0 & g(z_3) & \cdots & & & \\ \cdot & \cdot & \cdot & \cdot & \cdot & \cdot & \cdot \\ \cdot & \cdot & \cdot & \cdot & \cdot & \cdot & g(z_N) \end{pmatrix} \tag{12}$$

The z_i are taken at evenly spaced mesh points $z_i = i \cdot D/(N+1)$.

Next, find a vector $\bar{u}$ where

$$\bar{u} = \begin{pmatrix} u(z_1) \\ \cdot \\ \cdot \\ u(z_N) \end{pmatrix} \tag{13}$$

Then $\bar{u}_n$ will be an approximation to the desired eigenfunction w_n.

Eq. (10) can be rewritten as

$$B^{-1}D\,\bar{u} + \lambda^2\,\bar{u} = 0 \tag{14}$$

and notice that (14) is now just a matrix eigenvalue problem.

Rewriting agan, we have

$$-B^{-1}\,D\,\bar{u} = \lambda^2\,\bar{u} \tag{15}$$

and letting $A = -B^{-1}D$ Eq. (15) becomes

$$A\,\bar{u} = \lambda^2\,\bar{u} \tag{16}$$

where

$$A = \begin{pmatrix} \frac{2}{g(z_1)} & -\frac{1}{g(z_1)} & 0 & \cdot & \cdot & \cdot & \cdot \\ -\frac{1}{g(z_2)} & \frac{2}{g(z_2)} & -\frac{1}{g(z_2)} & 0 & \cdot & \cdot & \cdot \\ 0 & -\frac{1}{g(z_3)} & \cdot & \cdot & \cdot & \cdot & \cdot \\ \cdot & \cdot & \cdot & \cdot & \cdot & \cdot & \cdot \\ \cdot & \cdot & \cdot & \cdot & \cdot & -\frac{1}{g(z_N)} & \frac{2}{g(z_N)} \end{pmatrix} \tag{17}$$

Next Eq. (16) is solved numerically. Fortunately A is of simple form such that the solution of the equation

$$\det\,(A - \lambda^2 I) = 0 \tag{18}$$

is greatly simplified. In fact, for an arbitrary x, det(A-xI) can be evaluated in only about 3N operations, using a simple recursion formula (refer to Dahlquist and Bjorck, 1970).

Using bisection followed by the secant method, the first five roots of (18) can usually be found using less than a minute of computing time.

The equation

$$(A - \lambda_i^2 \ I)\ \bar{u}_i = 0 \tag{19}$$

is then solved for $i = 1,2,\ldots 5$. Since $\det(A - \lambda_i^2 \ I)=0$ (i.e. λ^2 is an eigenvalue), the solution (19) is not determined; however by setting

$$u_i(z_N) = 1/N \tag{20}$$

the remainder of the eigenvector $\bar{u}_i$ is uniquely determined. It should be noted that (20) is necessary because, in fact, the w_n of the original equation are unique only up to a multiplicative constant.

5.0 Mode Shape Perturbations

This study examines only the semi-diurnal tidal component of the internal wave field. As discussed earlier in this report the semi-diurnal component is the most energetic high frequency signal seen in the data (Fig. 2). The analyses of the vertical structure to follow were computed using the averaged Brunt-Väisälä profiles (refer to Table 2 and Fig. 4, Section 3.0) via the numerical method as given in Section 4.0.

When viewing the results to follow the reader should bear in mind the following.

1. By convention the modes were plotted in such a manner that the first maximum (nearest the surface) is always positive.
2. The vertical displacement is normalized to 1.0. For this study no energy mapping onto the modes was done. As such it is not possible at this time to assign the energy distribution by mode. From a cursory examination of the data it is felt, however, that because of the proximity to the continental shelf the lower order modes will dominate.
3. Only the first three modes are plotted. This is done partly for clarity and also because of the assumption of lower order mode dominance.

Figs. 5 through 9 present the mode structure for the five cases. To reiterate the cases are as follows.

1. Case 1 - period of onset of the meso-scale event.
2. Case 2 - period of greatest perturbing by the event.
3. Case 3 - period of passage.
4. Case 4 - quiescent period; no observable meso-scale feature.
5. Case 5 - minor perturbation but no indication of a meso-scale event.

In order to better examine the effect of the meso-scale feature the individual modes were compared to the quiescent case 4. Case 5 was not used in this comparison. Figs. 10 through 12 present the comparisons of modes 1, 2, and 3, respectively. The results are summarized as follows.

For mode 1 the level of maximum surfaces by of the order of 200 m during the period of greatest meso-scale perturbing. This is of particular importance in that the region of maximum occurs near the zone of the sound speed minimum. The maxima level change in the mode 2 cases also occurs in the region of the sound speed minimum. However, the perturbing effect is much greater; maxima surfacing by the order of 500 m. For the surface maximum there is no apparent level change but the amplitude of the maximum changes by approximately 25%. Again in the mode 3 comparisons there exist amplitude and level changes of the same order of magnitude.

In terms of the effects of these perturbations on the acoustic field the relationship is not completely known. First, as pointed out by Mooers (1975) the only simple

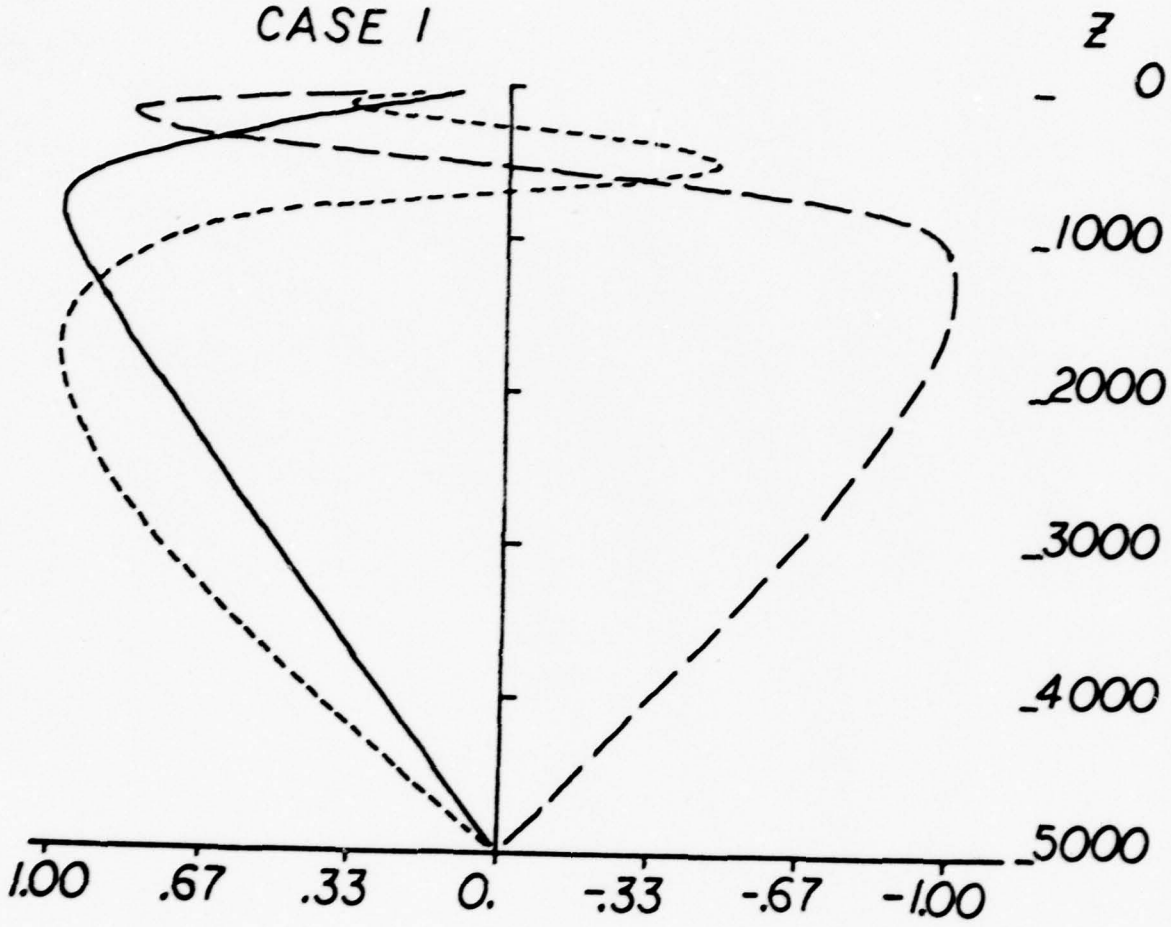

Fig. 5 Mode Structure: Case 1

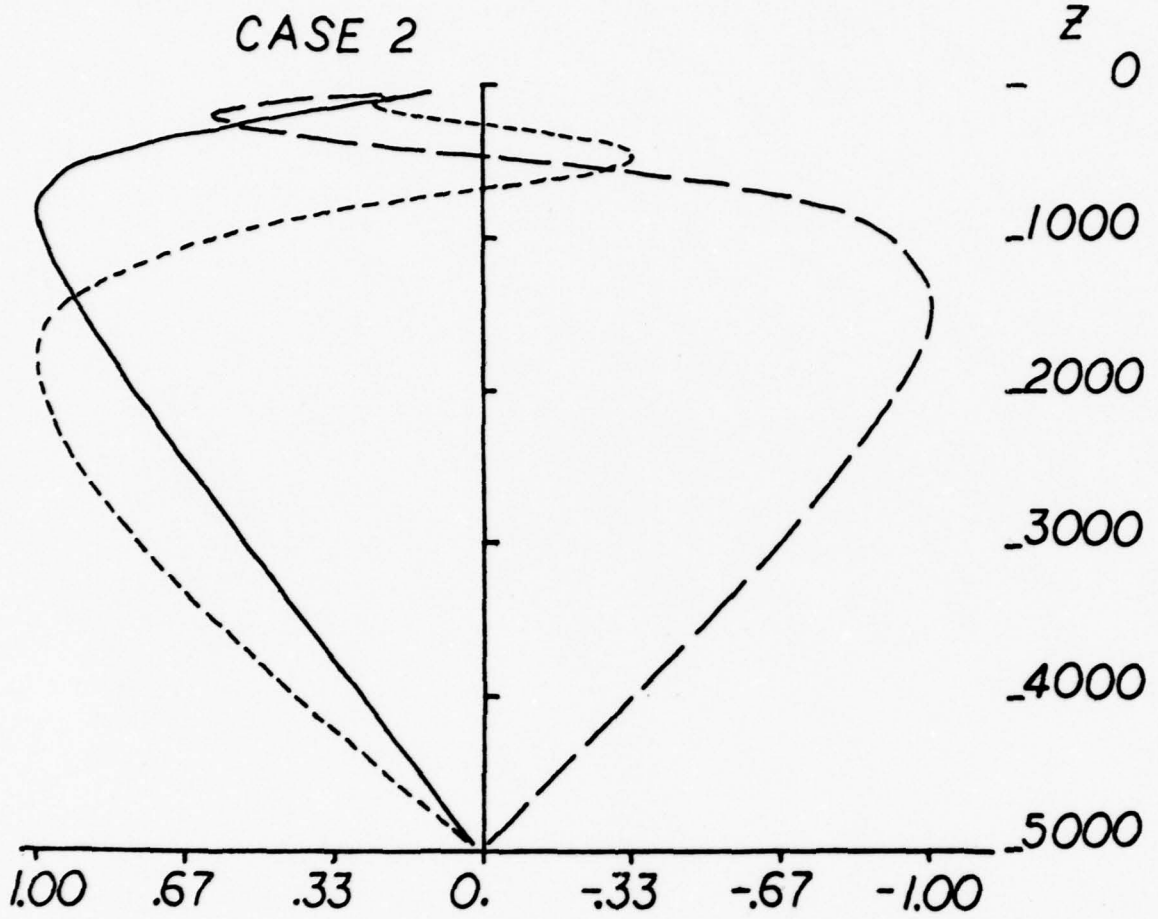

Fig. 6 Mode Structure: Case 2

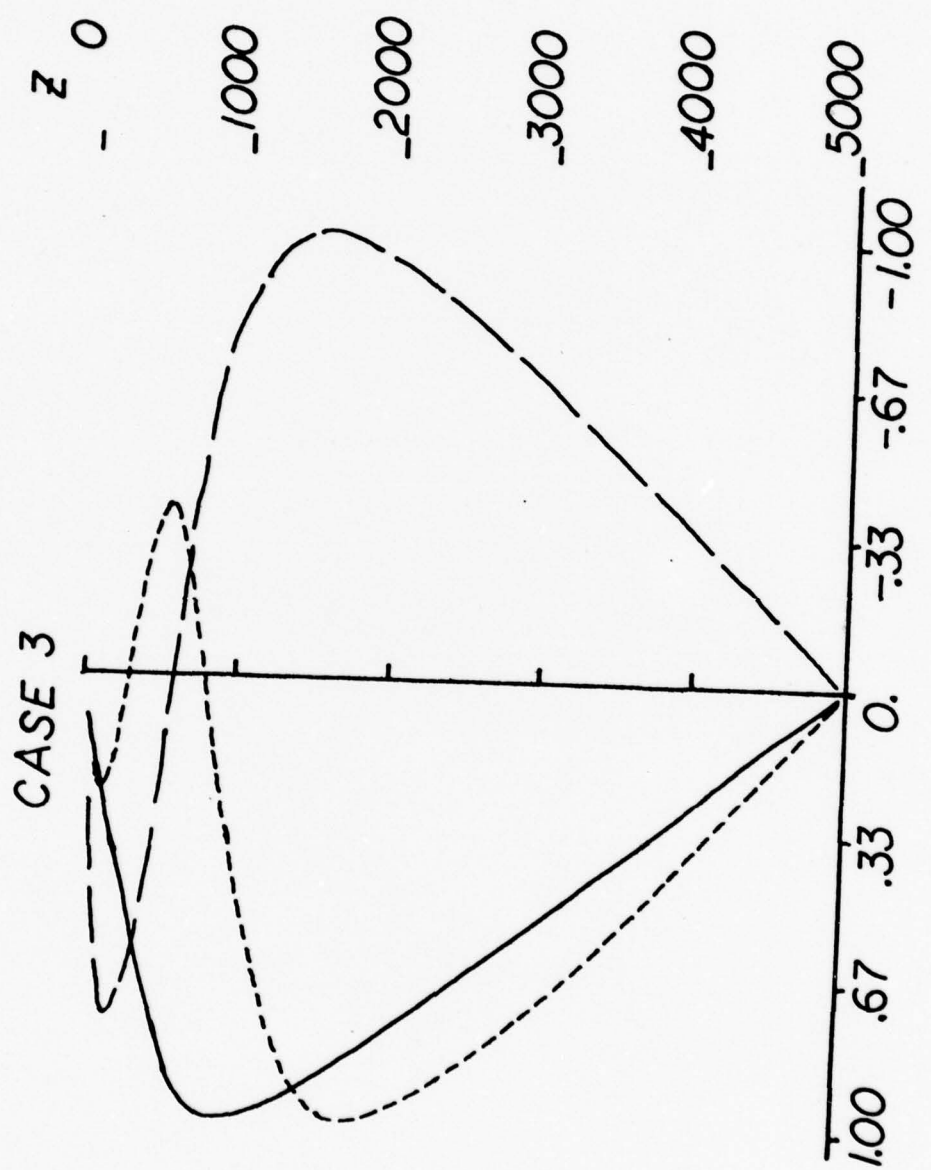

Fig. 7 Mode Structure: Case 3.

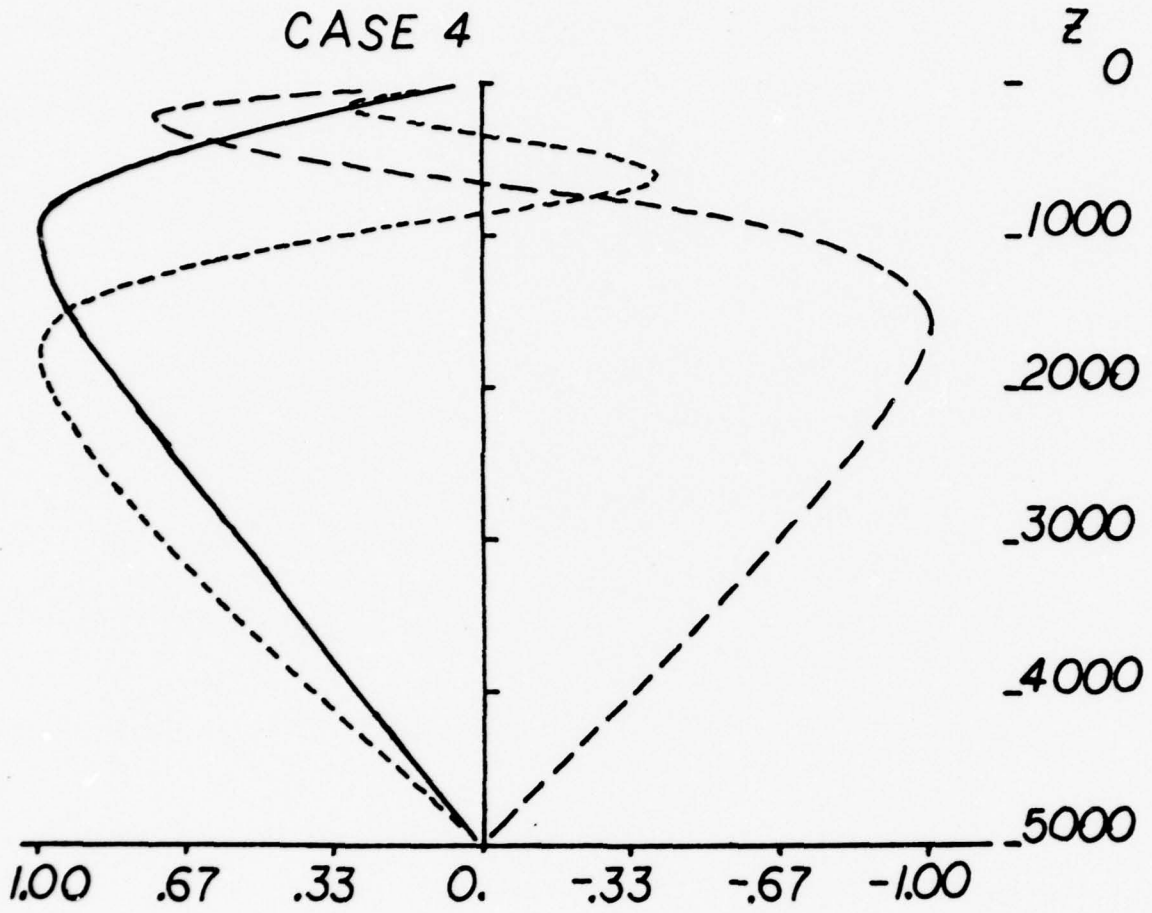

Fig. 8 Mode Structure: Case 4

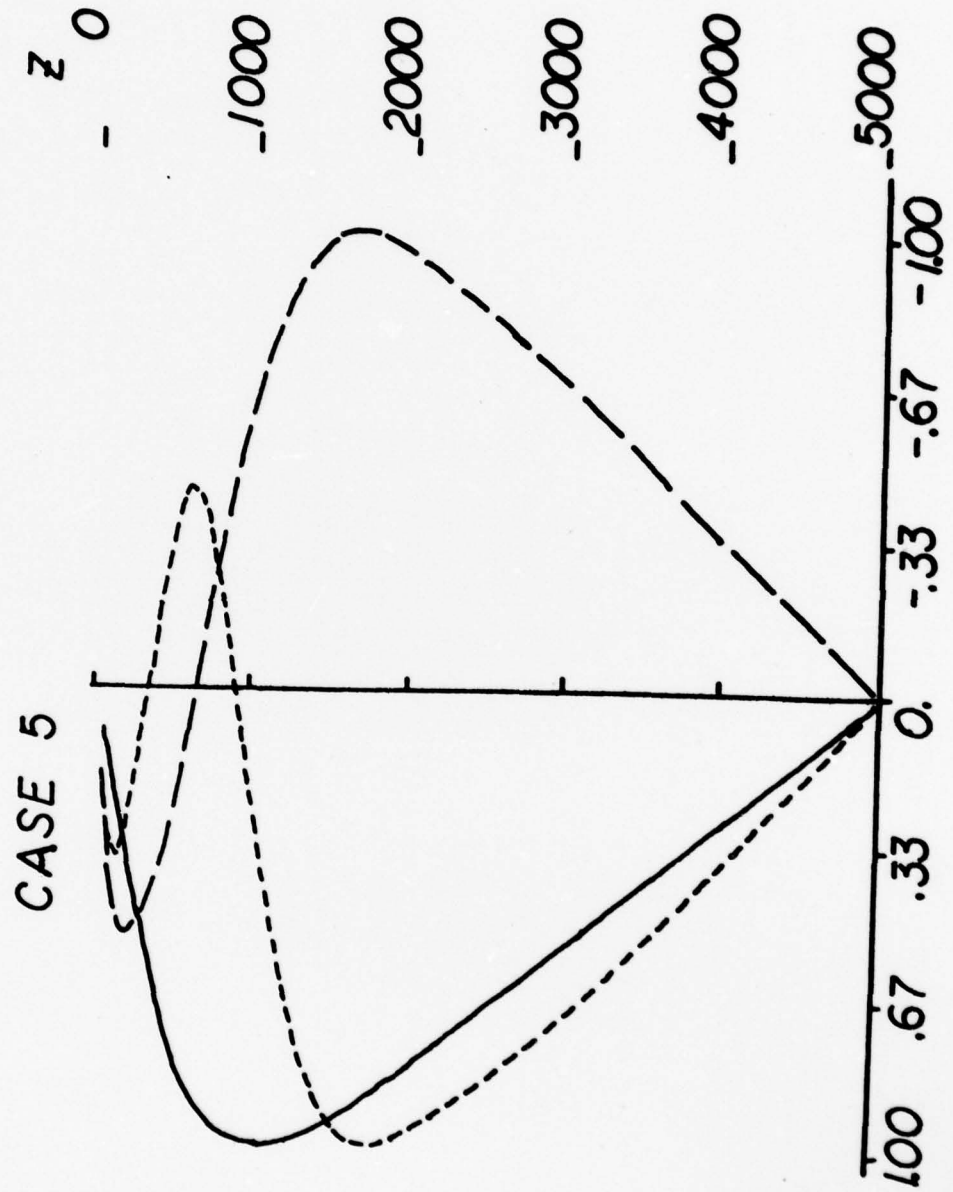

Fig. 9 Mode Structure: Case 5

relationship between a given mode structure and the corresponding sound speed anomaly is the depth of the zero crossings. Thus for the higher order modes the changes in level of the zero crossings (refer to the mode 2 and 3 cases, Figs. 11 and 12) will contribute to as yet unknown perturbations in the sound speed anomalies. Secondly, in general, variations in the depth of the SOFAR axis occur in response to and are approximately equal to the maximum amplitude of the first mode. However, the effect of the level change on SOFAR axis variations is new question.

Before the results of this study can be used to address the above questions the following must be done. The energy mapping onto mode must be done for the four cases; ie determine the energy partitioning. Once known it is then possible to examine the interference patterns in the sound speed anomalies and determine the effect of the meso-scale event.

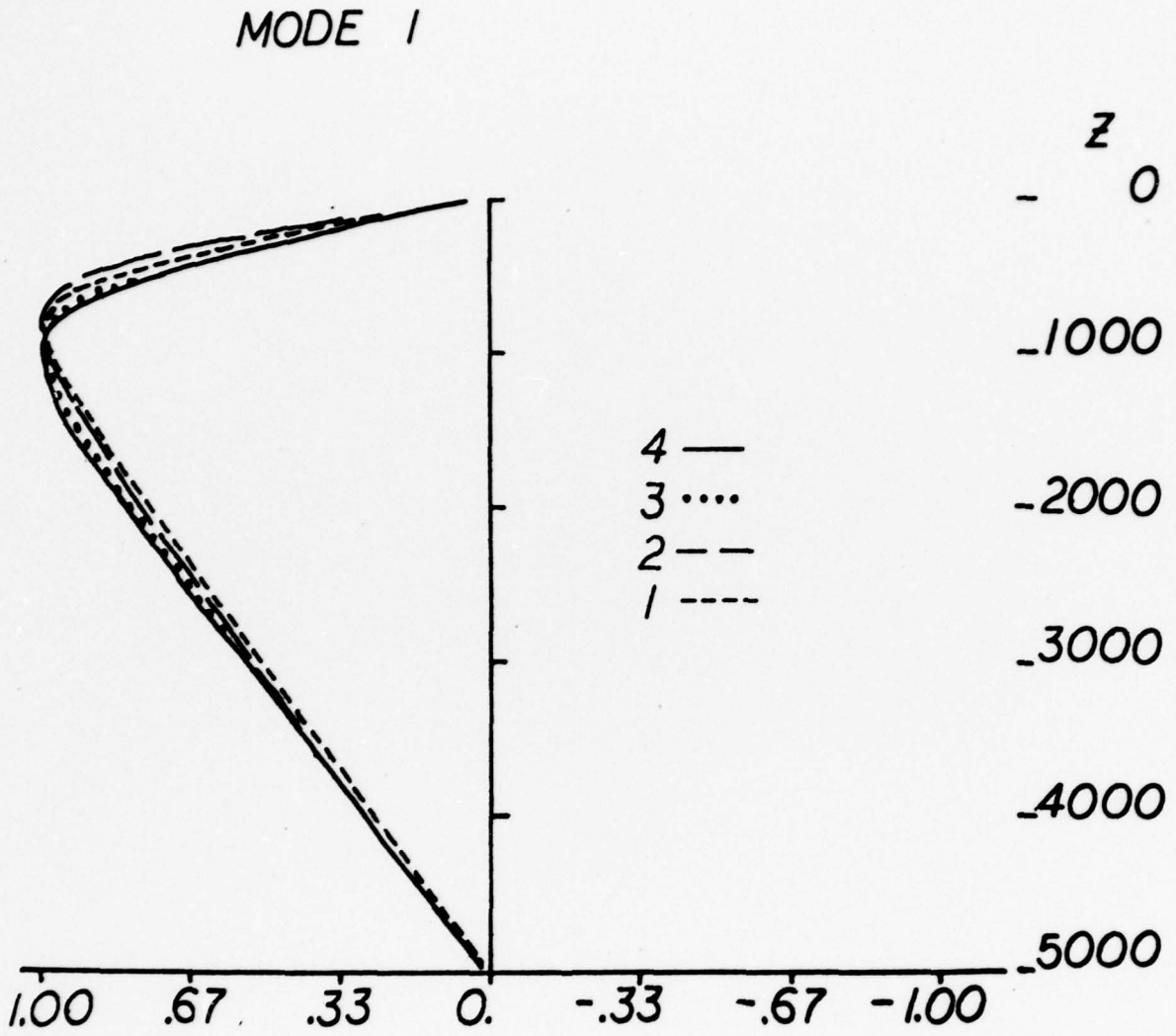

Fig. 10 Structure Comparison of Mode 1

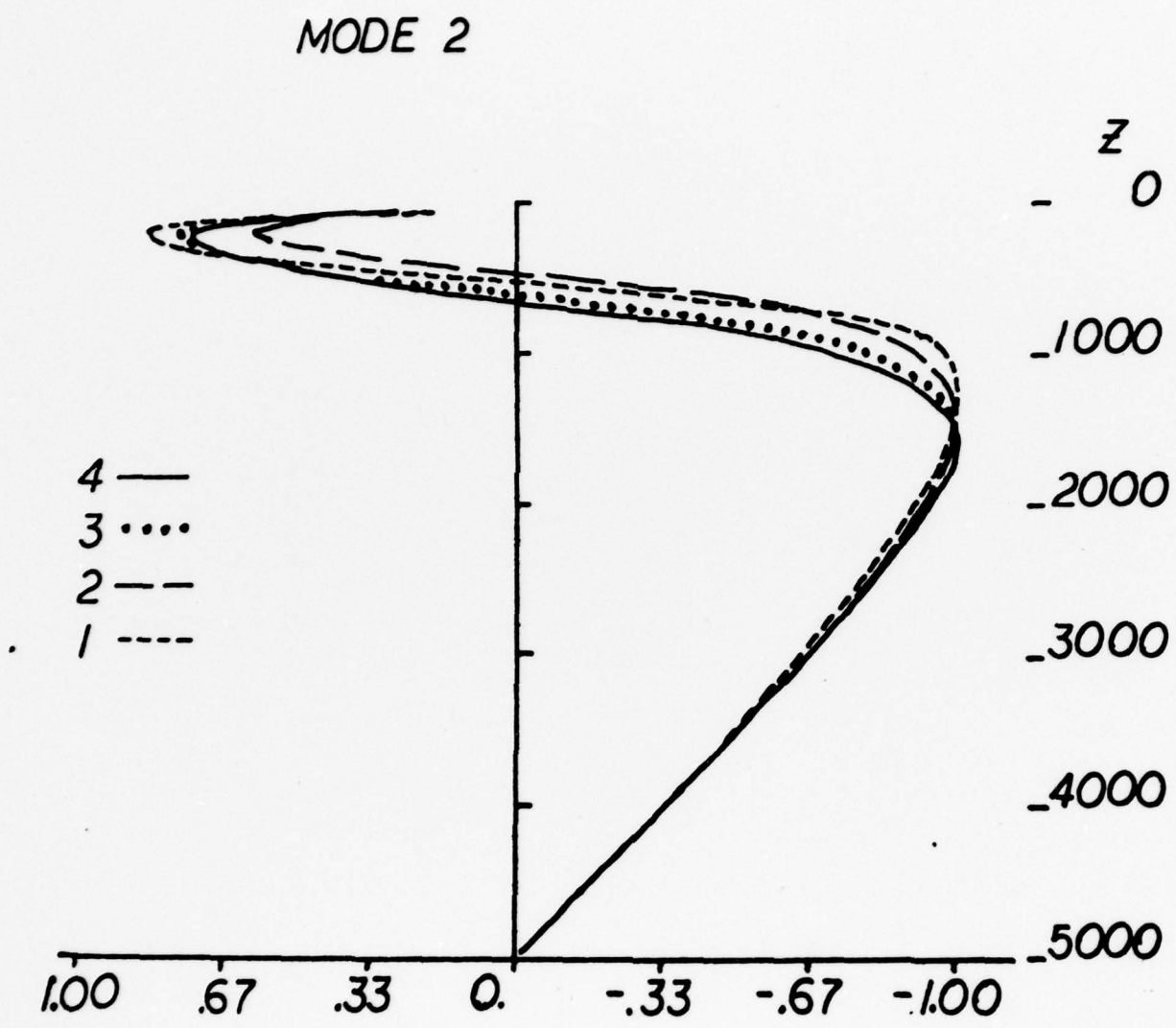

Fig. 11 Structure Comparison of Mode 2

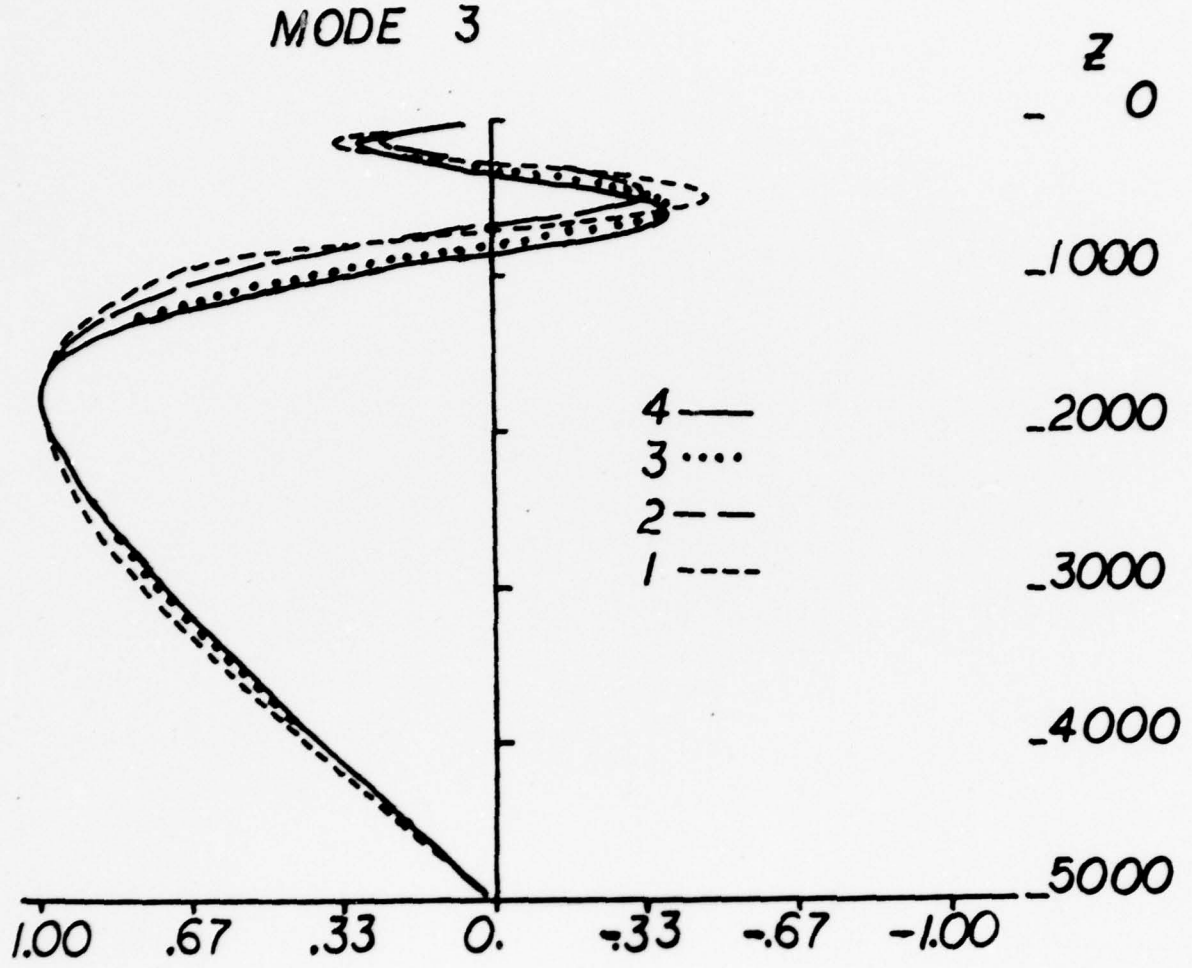

Fig. 12 Structure Comparison of Mode 3

6.0 Discussion

This study has presented changes in the vertical structure of the semi-diurnal tidal component of the internal wave field. The perturbations were associated with the passage of a meso-scale feature through the study region.

The results of this study have shown that the meso-scale feature had a decided influence on both the depth location and the amplitude of the maxima of the vertical displacement. These results are not surprising in that the amplitude and location of maxima are functions of the static stability. However, this reports documents, for the first time, this effect. The impact of these results is the magnitude of the perturbation on the mode structure. It should be remembered that the feature observed in these data was an edge effect. Thus much larger perturbations in the structure would be expected in the center of such a feature. Obviously these perturbations, considering the time scale, will have a direct effect on the acoustic path structure. But it should be emphasized that the acoustic problem cannot be treated until the total energy is partitioned by mode. Once that step is taken it is then possible to relate, in a quantitative manner, the effects of meso-scale features on the acoustic field.

REFERENCES

Dahlquist, G. and A. Bjorck, 1970: Numerical Methods. Prentice Hall, 573 pp.

Echternacht, K.L., 1976: BEAR Buoy: The engineering documentation for scientific application. IAR Report No. 76002.

_____, 1977: BEAR Buoy: The mooring configuration model and method used to correct sensors for vertical displacements. IAR Report No. 77008.

_____, 1978: BEAR Buoy: Analyses of acquired temperature data. IAR Report No. 78001.

Keller, H.B., 1968: Numerical Methods for Two-point Boundary-Value Problems. Blaisdell Pub Co., 184 pp.

Kronengold, M., 1976: BEAR: An environmental measurement buoy. Proc. of the 22nd Internat. Instrum. Sympos., San Diego, Cal., May 25-27, 1976.

Lai, D.Y. and P.L. Richardson, 1977: Distribution and movement of Gulf Stream rings. J. Phys. Oceanogr., 7, 670-683.

Mooers, C.N.K., 1975: Sound-velocity perturbations due to low-frequency motions in the ocean. J. Acoust. Soc. Am., 57, 1067-1075.

Phillips, O.M., 1966: The Dynamics of the Upper Ocean. Cambridge at the Un. Press, 261 pp.

DISTRIBUTION LIST

Office of Naval Research
800 N. Quincy Street
Arlington, Virginia 22217
Att: Code 222 — 2
1020S — 1
480 — 1

Director — 6
Naval Research Laboratory
4555 Overlook Avenue S.W.
Washington, D.C. 20375

Director — 1
Office of Naval Research Branch Office
1030 East Green Street
Pasadena, California 91106

Office of Naval Research — 1
San Francisco Area Office
760 Market Street Room 447
San Francisco, California 94102

Director — 1
Office of Naval Research Branch Office
495 Summer Street
Boston, Massachusetts 02210

Office of Naval Research — 1
New York Area Office
207 West 24th Street
New York, N.Y. 10011

Commanding Officer — 1
Office of Naval Research Branch Office
Box 39
FPO New York 09510

Director — 1
Office of Naval Research Branch Office
536 South Clark Street
Chicago, Illinois 60606

Commander — 1
Naval Surface Weapons Center
Acoustics Division
Silver Spring, Maryland 20910
Att: Dr. Zaka Slawsky

Naval Oceanographic Office — 1
NSTL Station
Bay St. Louis, Miss. 39520
Att: Mr. W. Geddes

Officer in Charge — 1
Naval Ship R&D Center
Annapolis Laboratory
Annapolis, Maryland 21402

Commander
Naval Sea Systems Command
National Center #2
2521 Jefferson Davis Highway
Arlington, Virginia 20360
Att: SEA 037 — 1
Carey Smith, 06H1 — 1
David F. Bolka, 06H2 — 1

Commanding Officer — 1
Fleet Numerical Weather Center
Monterey, Calif. 93940

Defense Documentation Center — 12
Cameron Station
Alexandria, Virginia 22314

Director of Navy Laboratories — 1
Chief of Naval Material
2211 Jefferson Davis Highway
Crystal Plaza #5
Arlington, Virginia 20360
Att: Dr. James Probus, MAT 03L

Commander — 1
Naval Electronic Systems Command
2511 Jefferson Davis Highway
National Center #1
Arlington, Virginia 20360
Att: CDR A.R. Miller, ELEX 320

Commander — 2
Naval Ship R&D Center
Dept. of the Navy
Bethesda, Maryland 20084
Att: Mr. Craig Olson
Uncl. Library

Chief of Naval Operations — 1
Room 4D518, Pentagon
Washington, D.C. 20350
Att: Capt. A.H. Gilmore

Commander — 3
Naval Ocean Systems Center
Dept. of the Navy
San Diego, Calif. 92132
Att: Dr. Dan Andrews
Dr. Dean Hanna
Mr. Henry Aurand

Superintendent 1
Naval Research Laboratory
Underwater Sound Reference Division
P.O. Box 8337
Orlando, Fla. 32806

Commanding Officer 3
Naval Underwater Systems Center
New London Laboratory
New London, Conn. 06320
Att: Dr. A. Nuttall
Mr. A. Ellinthorpe
Dr. D.M. Viccione

Commander 1
Naval Air Development Center
Dept. of the Navy
Warminster, Pennsylvania 18974
Att: Unclass. Library

Superintendent 1
Naval Postgraduate School
Monterey, Calif. 93940
Att: Unclass. Library

Commanding Officer 1
Naval Coastal Systems Laboratory
Panama City, Fla. 32401
Att: Unclass. Library

Commanding Officer 1
Naval Underwater Systems Center
Newport Laboratory
Newport, Rhode Island 02840
Att: Unclass. Library

Superintendent 1
U.S. Naval Academy
Annapolis, Maryland 21402
Att: Library

Commanding Officer 2
Naval Intelligence Support Center
4301 Suitland Road
Suitland, Maryland 20390
Att: Dr. Johann Martinek
Mr. E. Bissett

Commander 1
Naval Sea Systems Command
Washington, D.C. 20362
Att: Uncl. Library, SEA 03E

Special Assistant for ASW 1
Office of the Assistant Secretary of
the Navy for Research, Engineering
& Systems
Washington, D.C. 20350
Att: Dr. D. Hyde

Dr. Melvin J. Jacobson 1
Rensselaer Polytechnic Inst.
Troy, New York 12181

Dr. T.G. Birdsall 1
Cooley Electronics Laboratory
University of Michigan
Ann Arbor, Michigan 48105

Dr. Harry DeFerrari 1
University of Miami
Rosenstiel School of Marine Science
4600 Rickenbacker Causeway
Miami, Florida 33149

Dr. M.A. Basin 1
S.D.P. Inc
15250 Ventura Blvd
Suite 518
Sherman Oaks, Calif 91403

Dr. Walter Duing 1
University of Miami
Rosenstiel School of Marine Sciences
4600 Rickenbacker Causeway
Miami, Fla. 33149

Dr. David Middleton 1
127 East 91st Street
New York, N.Y. 10028

Dr. Donald Tufts 1
University of Rhode Island
Kingston, Rhode Island 02881

Dr. Loren Nolte 1
Duke University
Dept. of Electrical Eng.
Durham, N. Carolina 27706

Mr. S.W. Autrey 1
Hughes Aircraft Company
P.O. Box 3310
Fullerton, Calif. 92634

Dr. Richard W. James 1
c/o Fleet Weather Facility
4031 Suitland Rd.
Washington, D.C. 20390

Dr. Thomas W. Ellis 1
Texas Instruments, Inc.
13500 North Central Expressway
Dallas, Texas 75231

Dr. Terry Ewart 1
Applied Physics Lab.
University of Washington
1013 N.E. 40th Street
Seattle, Wash., 98195

Institute for Acoustical Research 2
Miami Div. of Palisades Geophysical Inst.
615 S.W. 2nd Avenue
Miami, Fla. 33130
Att: Mr. M. Kronengold
Dr. J. Clark
Dr. W. Jobst

Mr. Carl Hartdegen 1
Palisades Sofar Station
Bermuda Div. of Palisades Geophysical Inst.
FPO New York 09560

Mr. Beaumont Buck 1
Polar Research Lab.
123 Santa Barbara Avenue
Santa Barbara, Calif 93101

Dr. M. Weinstein 1
Underwater Systems Inc.
8121 Georgia Avenue
Silver Spring, Maryland 20910

Applied Research Laboratories 2
Univ. of Texas at Austin
P.O. Box 8029
10000 FM Road 1325
Austin, Texas 78712
Att: Dr. Lloyd Hampton
Dr. Charles Wood

Dr. C.N.K. Mooers 1
University of Delaware
Newark, Delaware 19711

Woods Hole Oceanographic Inst. 1
Woods Hole, Massachusetts 02543
Att: Dr. Paul McElroy

Dr. John Bouyoucos 1
Hydroacoustics, Inc.
321 Northland Avenue
P.O. Box 3818
Rochester, N.Y. 14610

Atlantic Oceanographic & Meteorological Lab.
15 Rickenbacker Causeway
Miami, Fla. 33149
Att: Dr. John Proni — 1

S.A.I. Inc.
8400 Westpark Drive
McClean, Virginia 22102
Att: Ms. Angela D'Amico
Ms. Lorna Blumer — 1

Commanding Officer
U.S. Naval Facility
FPO, New York 09556 — 1

Dr. Victor C. Anderson
Marine Physical Lab.
Scripps Inst. of Oceanography
University of California
La Jolla, Calif. 92037 — 1

Office of Naval Research
Resident Rep.
Lamont-Doherty Geological Observatory
Palisades, New York 10964 — 1

Advanced Research Projects Agency (ARPA)
1400 Wilson Blvd.
Arlington, Va. 22209
Att: Dr. R. Gustafson — 1

Naval Air Development Center
Warminster, Pa. 18974
Att: Keith Jerome, Proj. Eng. — 1

Ocean Systems Pacific
Box 1309
FPO San Francisco 96610
Att: LCDR F.T. Gray
Lt. William Johnston — 1

Commander Oceanographic Systems Atlantic (COSL)
Box 100
Norfolk, Va. — 1

NORDA
NSTL Station
Bay St. Louis, Miss., 39520
Att: M.G. Lewis — 1

SECURITY CLASSIFICATION OF THIS PAGE (When Data Entered)

REPORT DOCUMENTATION PAGE		READ INSTRUCTIONS BEFORE COMPLETING FORM
1. REPORT NUMBER 78004	2. GOVT ACCESSION NO.	3. RECIPIENT'S CATALOG NUMBER
4. TITLE (and Subtitle) BEAR Buoy Study: Internal Wave Mode Perturbations due to the Passage of a Mesoscale Feature		5. TYPE OF REPORT & PERIOD COVERED 2 October to 27 Oct 1978 Final Report 6. PERFORMING ORG. REPORT NUMBER
7. AUTHOR(s) Kenneth L. Echternacht		8. CONTRACT OR GRANT NUMBER(s) 74-C-0229 N00014-~~77-C-0446~~
9. PERFORMING ORGANIZATION NAME AND ADDRESS Institute for Acoustical Research 615 S.W. 2nd Avenue Miami, Florida 33130		10. PROGRAM ELEMENT, PROJECT, TASK AREA & WORK UNIT NUMBERS
11. CONTROLLING OFFICE NAME AND ADDRESS Procuring Contracting Officer Office of Naval Research, Dept. of the Navy, Arlington, Va. 22217		12. REPORT DATE Nov. 1978 13. NUMBER OF PAGES
14. MONITORING AGENCY NAME & ADDRESS (if different from Controlling Office) Office of Naval Research Resident Rep. Columbia University Lamont Doherty Geological Observatory Torrey Cliff, Palisades, N.Y. 10913		15. SECURITY CLASS. (of this report) Unclassified 15a. DECLASSIFICATION/DOWNGRADING SCHEDULE

16. DISTRIBUTION STATEMENT (of this Report)

Distribution of this Document is unlimited

17. DISTRIBUTION STATEMENT (of the abstract entered in Block 20, if different from Report)

18. SUPPLEMENTARY NOTES

19. KEY WORDS (Continue on reverse side if necessary and identify by block number)

Internal waves
vertical structure
mode structure
mesoscale eddy influence

20. ABSTRACT (Continue on reverse side if necessary and identify by block number)

This study examines, in detail, the effect of the passage of a meso-scale feature through an area normally under the influence of the Antilles Current. The study area lies approximately 40 km northeast of the island of Eleuthera, Bahamas. The analyses examine, in particular, changes in structure of the vertical displacements of the semi-diurnal tidal component of the internal wave field. The report also includes a description of the

DD FORM 1 JAN 73 1473 EDITION OF 1 NOV 65 IS OBSOLETE S/N 0102-014-6601

UNCLASSIFIED

Cont'd page

SECURITY CLASSIFICATION OF THIS PAGE (When Data Entered)

methodology used to compute the vertical displacements.